180
8-11-75

02-1533

UCRL-51830

AN EXAMINATION OF THE GEOLOGY AND SEISMOLOGY ASSOCIATED WITH AREA 410 AT THE NEVADA TEST SITE

W. J. Hannon
H. L. McKague

May 23, 1975

Prepared for U.S. Energy Research & Development Administration under contract No. W-7405-Eng-48

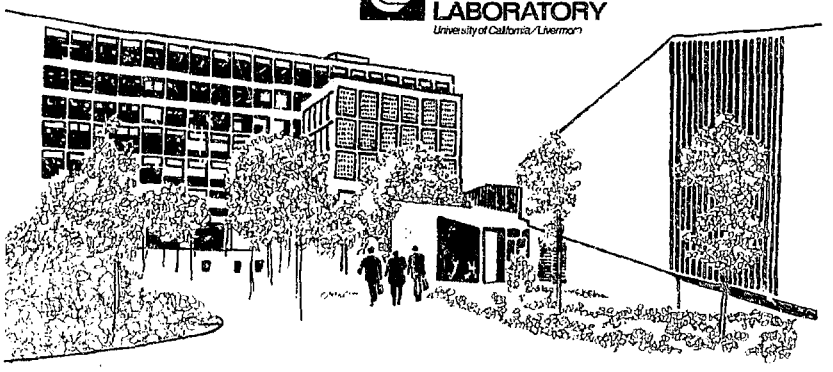

Printed in the United States of America
Available from
National Technical Information Service
U. S. Department of Commerce
5285 Port Royal Road
Springfield, Virginia 22151
Price: Printed Copy $___*; Microfiche $2.25

*Pages	NTIS Selling Price
1-50	$4.00
51-150	$5.45
151-325	$7.60
326-500	$10.60
501-1000	$13.60

Distribution Category
UC-11

LAWRENCE LIVERMORE LABORATORY
University of California/Livermore, California/94550

UCRL-51830

AN EXAMINATION OF THE GEOLOGY AND SEISMOLOGY ASSOCIATED WITH AREA 410 AT THE NEVADA TEST SITE

W. J. Hannon

H. L. McKague

MS. date: May 23, 1975

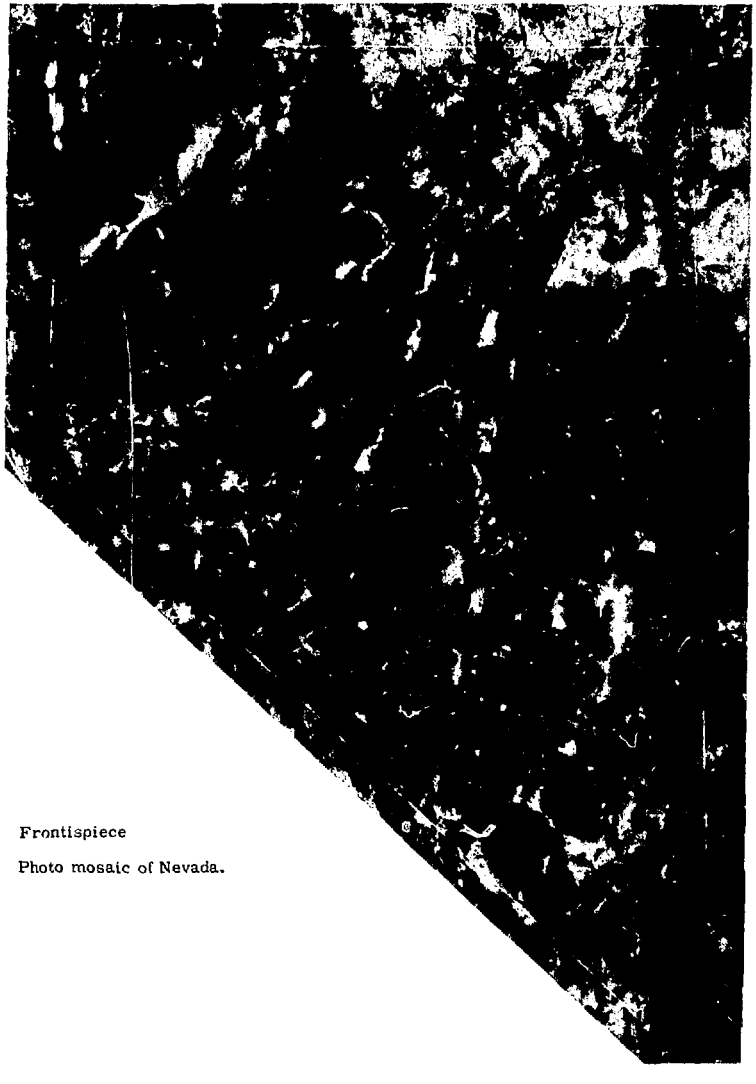

Frontispiece

Photo mosaic of Nevada.

Contents

AN EXAMINATION OF THE GEOLOGY AND SEISMOLOGY ASSOCIATED WITH AREA 410 AT THE NEVADA TEST SITE

Abstract

This report summarizes regional and local geology at the Nevada Test Site and identifies major tectonic features and active faults. Sufficient information is given to perform seismic safety analyses of present and future critical construction at the Super Kukla Site and Sites A and B in Area 410. However, examination of local minor faults and joints and soil thickness studies should be undertaken at construction time. The Cane Spring Fault is identified as the most significant geologic feature from the viewpoint of the potential seismic risk. Predictions of the peak ground acceleration (0.9 g), the response spectra for the Safe Shutdown Earthquake, and the maximum displacement across the Cane Spring Fault are made.

Introduction

ERDA has requested that LLL investigate the earthquake hazard for critical facilities at the Livermore site, Site 300, and Area 41C at the Nevada Test Site (NTS). A safety analysis is needed because facilities containing radioactive materials are located in these areas. This report examines the geology and seismicity of the Super Kukla Reactor Site and Sites A and B in Area 410.

The geological investigations consist of summaries of the regional and local geologic history, past and present tectonic features, and regional and local stratigraphy. Active faults were identified on the basis of geology, surficial expression, seismicity, and the stress state of the region. The Cane Spring Fault was identified as the most significant feature on the basis of its length and its proximity to the facilities being studied.

Once the active faults were identified, their dimensions and prior seismic history were used together with the results of previous investigations to predict acceleration levels. Two different prediction schemes were used depending on whether the nearest point on the fault was greater or less than 5 km from the building sites. In the former case, the predictions were based on the results of empirical observations of peak accelerations versus distance for a given magnitude and on studies of magnitude versus fault length. In the latter case, the prediction scheme was based upon close-in observations made during the 1966 Parkfield earthquake and the 1971 San Fernando earthquake. These were suitably scaled on the basis of estimated peak acceleration.

The results of the analysis show that the Cane Spring Fault is the primary

seismic hazard. A peak acceleration of 0.9 g is assigned to this fault and 0.2-0.5 m is estimated as the maximum displacement to be expected across the fault. The corresponding response spectra are determined.

Regional Geology

NTS is located within the south central part of the Great Basin section of the Basin and Range physiographic province (Fig. 1).[1] This province is characterized by a series of linear north to northeast trending mountain ranges (frontispiece and Fig. 2).[1] The ranges, which rise to heights of 2100 to 3100 m, are separated by intermountain basins at elevations of 900 to 1500 m.

In general, the rocks of the Basin and Range Province can be characterized as metamorphic rocks of Early Precambrian age [1640 m.y. (million years)][2]; sedimentary rocks of Late Precambrian (850 m.y.),[3] Paleozoic, and Mesozoic age; plutonic rocks of Mesozoic and Tertiary age; and volcanic and sedimentary rocks of Cenozoic age.

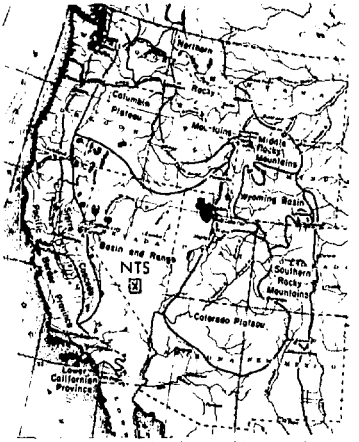

Fig. 1. Map of physiographic provinces of the Western United States.[1] (From Physiography of the United States by Charles B. Hunt, W. H. Freeman and Company. Copyright © 1967.)

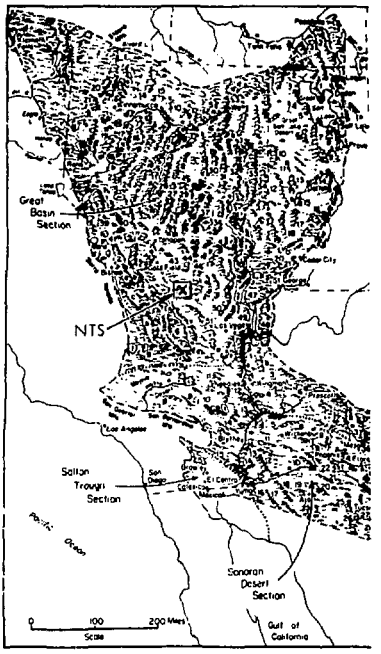

Fig. 2. Physiographic map of the Basin and Range Province.[1] (From Physiography of the United States by Charles B. Hunt, W. H. Freeman and Company. Copyright © 1967.)

The crust of the basin is relatively thin, averaging about 15 km thick. In Mesozoic time, complex thrusting and folding occurred and a number of granitic plutons were intruded. In the Tertiary period,[4] a change to extensional deformation occurred giving rise to three general groups of interrelated structures: (1) block faulting, (2) major zones of strike-slip faulting, and (3) volcano-tectonic features.[5]

GEOLOGIC HISTORY

The older Precambrian rocks are highly metamorphosed sedimentary and igneous rocks, now represented by scattered occurrences of schists, gneisses, and marbles. These rocks were involved in the Hudsonian orogeny (1640-1680 m.y.).[2] The overlying Upper Precambrian rocks are relatively unmetamorphosed sedimentary and volcanic rocks.[3] These rocks are divided into two series. The lower series ranges from 850-1250 m.y. in age. The upper series is 850 m.y. old and cannot be consistently separated from the Lower Cambrian rocks. The depositional pattern of the upper series departs from that of older rocks but is similar to the pattern of younger rocks deposited in the Cordilleran geosyncline. Stewart[3] proposes that this represents a change in tectonic setting and that these Upper Precambrian to Lower Cambrian rocks (570 to 850 m.y.) were the initial deposits in the Cordilleran geosyncline.

The rocks of Cordilleran geosyncline can most simply be divided into a eugeosynclinal group of clastic sedimentary rocks to the west of a group of miogeosynclinal, predominantly carbonate rocks. The NTS is near the thickest section of the miogeosyncline.[6] The eastern boundary of the eugeosyncline lies about 80 km west of the NTS [Figs. 3 (Ref. 7) and 4]. The miogeosynclinal sequence is largely Paleozoic rocks with some remnants of Lower Mesozoic rocks at the top.[2]

The rocks in the vicinity of the NTS may be roughly described as follows: the oldest rocks consist of a 1500-m-thick Precambrian and Lower Cambrian sequence of clastic rocks. These clastic rocks underlie a 4600-m-thick Middle Cambrian to Middle Devonian carbonate sequence. The Eleana Formation, a 2400-m-thick clastic sequence of Upper Devonian and Mississippian age rocks, overlies the lower carbonate sequence. The Eleana Formation, in turn, is overlain by an 1100-m-thick carbonate sequence of Pennsylvanian-Permian age. A stratigraphic column for the pre-Mesozoic rocks at NTS and vicinity is given in Table 1.[8, 9]

REGIONAL DEFORMATION AND VOLCANISM

The rocks of the eugeosyncline to the west were deformed by the Antler orogeny of early Mississippian time (340 m.y.). This orogeny occurred northwest of NTS and is represented at the test site by the Eleana Formation. The Antler orogeny appears to have had a minimal structural effect on the miogeosynclinal rocks in the vicinity of NTS. However, after the deposition of the upper carbonate sequence, compressional deformation occurred in the Mesozoic era (Fig. 5). According to Barnes and Poole,[10] folding was preceded, accompanied, and followed by southeastward thrusting. They propose that the

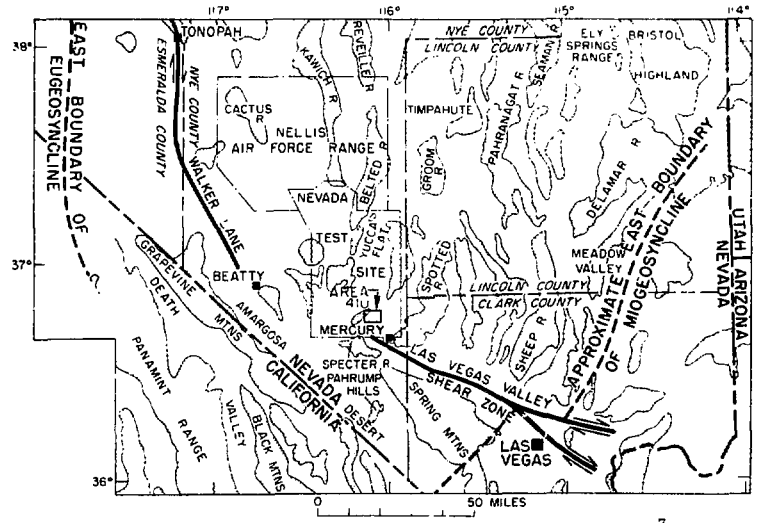

Fig. 3. Map showing extent of Cordilleran Geosyncline in vicinity of NTS.[7] (From Refs. 6 and 7. U. S. Geological Society of America.)

Table 1. Pre-Mesozoic Stratigraphic column for NTS and vicinity.

Geologic age	Geologic unit	Thickness (m)
Mississippian	Keeler Canyon Formation	65
	Red Spring Shale	120
	Perdido Formation	182
	Tin Mountain	91
Devonian	Lost Burro Formation	455
Silurian	Hidden Valley Dolomite	395
Ordvician	Ely Springs Dolomite	167
	Eureka Quartzite	100
	Pogonip Group	516
Cambrian	Nopah Formation	500
	Bonanza King Formation	1080
	Carrara Formation	405
	Zabriskie Quartzite	306
Precambrian	Wood Canyon Formation	680
	Stirling Quartzite	490
	Johnnia Formation	710
	Noonday dolomite and equivalent basinal units	330
	Kingston Peak Formation	1080
	Beck Spring Dolomite	340
	Crystal Spring Formation	1010

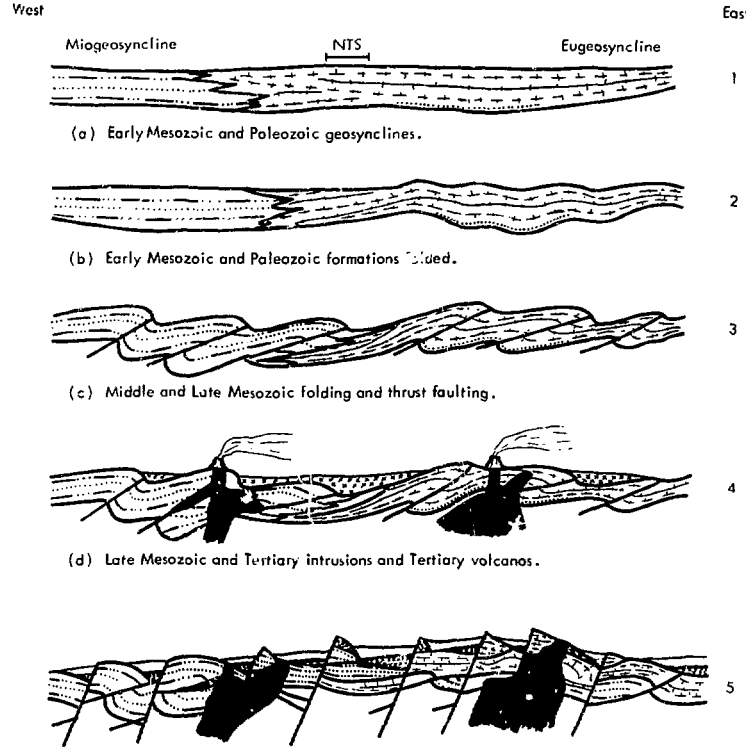

Fig. 4. Generalized evolution of structure and topograph in the vicinity of NTS.[1] (From Physiography of the United States by Charles B. Hunt. W. H. Freeman and Company. Copyright © 1967.)

root zone of the thrusts lies to the northwest of Yucca Flat.

Several episodes of Mesozoic thrusting have been recognized. Burchfield et al.[11] recognized a period of Jurassic (165 ± 4 m.y. and possibly 213 m.y.) thrust faulting in southeastern California, which they correlated with the thrusting observed at the NTS. Another episode of thrusting occurred between 75 and 90 m.y. ago in the Spring Mountains southeast of NTS.[12] King[2] notes that the Mesozoic deformation is progressively younger eastward across the foldbelt. Also, he noted that there is no clear separation between Middle Mesozoic and Late Mesozoic orogenies.

Starting approximately 26 m.y. ago,[4] the central part of the Cordillerian geosyncline was disrupted by block faulting resulting from extensional deformation. According to King,[2] major faulting occurred as recently as the early Pleistocene with minor faulting continuing today in places. It has been suggested by

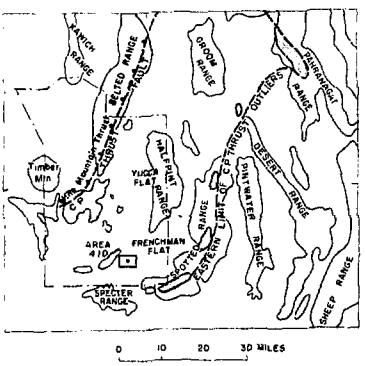

Fig. 5. Map showing Mesozoic thrust faults in NTS and vicinity.

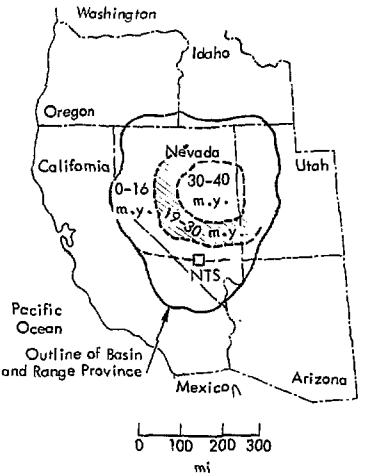

Fig. 6. Age distribution of Tertiary volcanism in Nevada.

Stewart[13] that the tensional deformation is the result of right lateral movement between the North American Plate and the Pacific Plate along the San Andreas and related faults. It is thought that the movement produces tensional fragmentation (Basin and Range structure) oblique to the trend of the plate boundaries.

An extensive period of volcanism started about 40 m.y.[14] and continued up until at least 3.25 m.y.[15] The oldest volcanic rocks occur most commonly in east central Nevada with the younger rocks occurring peripherally around the older center [Fig. 6 (Ref. 16)]. In addition, the older rocks are acidic in composition (andesite to rhyolite) while the youngest rocks are predominantly mafic (basalt). The acidic rocks are the most prevalent volcanic rocks in the vicinity of NTS.

NTS Geology

GENERAL GEOLOGY

The geology of NTS can be broadly divided into (1) a basement of compressively deformed Upper Precambrian and Paleozoic sedimentary rocks, (2) an overlying section of Tertiary and Quaternary volcanic rocks which are broken up by normal faulting, and (3) Late Tertiary and Quaternary alluvium and colluvium cut by normal faulting.

As noted before, the Precambrian and Paleozoic miogeosynclinal rocks at NTS can be divided into four groups. They are: (1) an Upper Precambrian and Lower Cambrian clastic sequence in which quartzite predominates, (2) a Middle Cambrian through Middle Devonian carbonate sequence, (3) the Devonian and Mississippian Eleana Formation composed of argillites and quartzites, and (4) a sequence of late Paleozoic carbonates (see Table 1).

DEFORMATION AND VOLCANISM

During the Paleozoic and Mesozoic eras, these rocks were subjected to several periods of compressive deformation. At NTS, the Mesozoic deformation resulted in the formation of folds and thrust faults (Fig. 4 b, c). The major thrust faults formed were the C. P. Thrust and the associated Mine Mountain Thrust (Fig 5).

The C. P. and Mine Mountain Thrust Faults are generally characterized by Upper Precambrian and Lower Paleozoic rocks overlying Middle and Upper Paleozoic rocks. Subsequently, the thrusts were cut by later normal faulting and have not been active in the Tertiary. (Fig. 4)

The Precambrian-Paleozoic rocks were locally intruded by Mesozoic plutonic rocks (Fig. 4d). Two small, predominantly quartz, monzonite stocks, the Gold Meadows stock and the Climax stock, are exposed in the northern part of NTS. They have an average K-Ar age of 93 ± 5 m.y.[17]

Tertiary volcanic rocks form a composite sequence over 12,190 m thick.[17] These volcanic rocks, especially the pre-Upper Miocene formations, are irregularly distributed as a result of preexisting topographic erosion and subsequent structural deformation. The Upper Miocene tuffs of Crater Flat (13.8 ± 0.4 m.y.) are the oldest widespread units at NTS. The younger volcanic units are easier to correlate over long distances. The general stratigraphy of the volcanic rocks is given in Table 2.

The oldest volcanic rocks at NTS occur within the Oligocene (29 m.y.) Horse Springs Formation. The location of the volcanic center or centers from which this and other older tuffs originated is unknown. The tuffs and lavas on the NTS of Late Miocene and Pliocene age are from volcanic centers within and near the NTS (Fig. 7). Table 3 summarizes the data for those volcanic centers of interest. There appears to be a close relationship between volcanism and normal faulting both in time and space.[5] Carr[5] believes there is an association of eruptive centers and calderas with the intersection of right-lateral shear zones and northeast trending faults.

Table 2. Generalized stratigraphic column of Tertiary volcanic rocks at NTS.[17]

Unit	General lithology	Volcanic center
Thirsty Canyon Tuff	Peralkaline ash-flow tuffs	Black Mountain Caldera
Labyrinth Canyon Member Gold Flat Member Trail Ridge Member Spearhead Member		
Timber Mountain Tuff	Rhyolitic to quartz-latitic ash-flow tuffs	Timber Mountain Caldera
Ammonia Tanks Member Rainier Mesa Member		
Paintbrush Tuff	Rhyolitic to quartz-latitic ash-flow tuffs	Claim Canyon Caldera
Tiva Canyon Member Yucca Mountain Member Pah Canyon Member Topopah Spring Member		
Lavas of Scrugham Peak Quadrangle (interbedded with Paintbrush tuff)	Rhyolitic lavas	Local centers on south side Pahute Mesa
Wahmonie Formation Salyer Formation	Dacitic to rhyodacitic lavas, breccias, tuffs, and sandstones	Wahmonie Flat-Mt. Salyer
Stockade Wash Tuff	Calcalkalic rhyolitic ash-flow tuff	Silent Canyon Caldera
Tuffs and rhyolites of Area 20		
Belted Range Tuff	Peralkaline ash-flow tuffs	
Grouse Canyon Member Tub Spring Member		
Rhyolite lavas of Quartet Dome (interbedded with lavas and ash-flow tuffs from Silent Canyon Caldera	Rhyolitic lavas	Localized centers around Silent Canyon Caldera
Crater Flat Tuff	Low-silica rhyolitic ash-flow tuffs	Sleeping Butte Caldera in north west part of Timber Mountain Caldera Complex
Older Ash-Flow Tuffs	Rhyolitic to dacitic tuffs	North of NTS

The extension which produced the north to northeast trending normal faulting began between 14 and 17 m.y. ago[4] and is probably continuing today. At NTS, two normal fault systems are present (Fig. 8). The older set strikes northeast and northwest. This system appears to have formed during or shortly after the extrusion of the oldest tuffs. This is based on the observation that the frequencies of

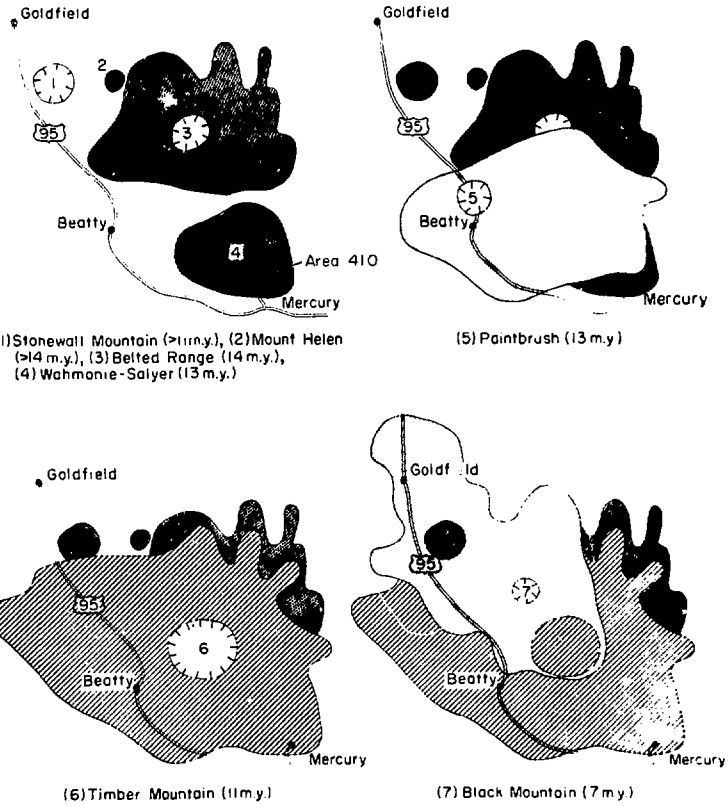

Fig. 7. Maps showing seven volcanic centers and five of the ash-flow tuff sheets that have been delimited in and adjacent to the NTS. (From Ref. 6, U. S. Geological Society of America.)

faulting in the older tuffs (>17 m.y.) and the pre-Tertiary rocks are similar. The older faulting appears to have ceased between 17 and 14 m.y. ago.

The younger fault set strikes north-south. This phase of faulting appears to have begun between 17 and 14 m.y. ago and is probably still continuing. For

Table 3. Summary of information for volcanic centers on and near NTS.

Volcanic center	Location	Associated lithologic unit	Age (m.y.)	Chemistry
Black Mountain	8 km west of NTS	Thirsty Canyon Tuff	7.5-6.2	Peralkaline
Timber Mountain	On western border of NTS	Timber Mountain Tuff	11.3-9.5	Calc-alkalic
Claim Canyon	35 to 40 km west of NTS in vicinity of Beatty, Nevada	Paintbrush Tuff	13.4-12.4	Calc-alkalic
Wahmonie-Salyer	6 km northwest of Area 410, NTS	Wahmonie Formation	12.5-12.9	Calc-alkalic
Silent Canyon	Beneath eastern Pahute Mesa, NTS	Belted Range Tuff	14.8-13.1	Peralkaline

example, the fault scarp along the Yucca Fault indicates its Recent Age. It is these faults with their north-south orientation that control the position and orientation of the present day basins and ranges.

The west-northwest-striking right-lateral Las Vegas Shear Zone is located just south of Mercury, Nevada (Fig. 3).

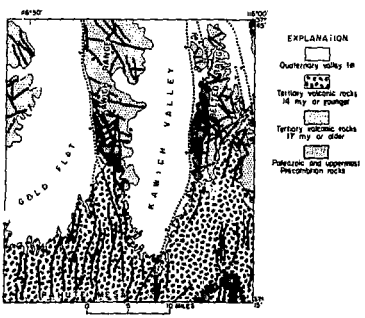

Fig. 8. Geologic map of the Belted and Kawich Ranges. (From Ref. 4. U.S. Geological Society of America publication.)

It is a major linear feature in southern Nevada. Because the north-striking ranges assume a more northeastwardly strike as they approach the Las Vegas Shear Zone, it seems reasonable that much of the movement along it has taken place since 17 m.y. In the Frenchman Mountain block east of Las Vegas, it appears that movement along the Las Vegas Shear Zone ended 11 m.y. ago.[18] Thus, much of the movement along the Las Vegas Shear Zone may have been restricted to a 6 m.y. period. Based on Longwell's[18] estimate of 67 km of lateral displacement along the zone, the displacement would be on the order of 1.1 cm/yr. This is in agreement with Stewart's estimate,[13] based on the geometry of block faulting, of 0.3 to 1.5 cm/yr. Southwest of Mercury in the Specter Range, the Las Vegas Shear Zone loses definition. Its extent and location to the northwest is unclear. Associated with the Las Vegas Shear Zone are several northeast-striking faults with left-lateral displacement ranging up to 5 Km. The Cane Spring Fault is one of these.

The final elements in the NTS geologic picture are the Late Tertiary and Quaternary alluvium- and colluvium-filled basins. Because they are structurally controlled by the north-south striking later fault systems, they must have developed and been filled with alluvium in the last 17 m.y. In some basins the alluvial fill is in excess of 1060 m thick. Several ages of alluvium have been recognized. A general stratigraphic column for alluvium-colluvium is given in Table 4. Some faults were contemporaneous with and/or postdated the younger alluvium. The Yucca Fault is an example.

GEOLOGY OF AREA 410

Area 410 is located in the southern part of NTS, near the southern boundary of the Southern Nevada Volcanic Field. The area falls within four geologic quadrangle maps. They are the Cane Spring Quadrangle,[19] the Skull Mountain Quadrangle,[20] the Camp Desert Rock Quadrangle,[21] and the Specter Range NW Quadrangle.[22] Within Area 410, the rocks are predominantly Tertiary tuffs and tuffaceous sediments and Tertiary or younger basalts, alluvium, and colluvium (Fig. 9).

Area 410 is southeast of the Wahmonie-Salyer Volcanic Center (Fig. 9). Most of the rock within this area is from that center. The older Salyer Formation occurs in the northeastern part of Area 410, while the younger Wahmonie Formations occurs over much of the remaining area. The Ammonia Tanks Formation overlies these older formations unconformably in some areas.

Cane Spring Wash and some of the hillsides are mantled with alluvium and/or colluvium of various ages. The older gravels are commonly more indurate than the younger alluvium. Alluvium and colluvium of at least four different ages have been recognized.[23] The oldest underlies the basalt of Skull Mountain. This is in turn unconformably overlain by alluvium and colluvium composed of boulders of Wahmonie lava and basalt of Skull Mountain. This alluvium is inferred by Ekren[23] to be either Late Tertiary or Very Early Quaternary. The basis for this inference is the amount of erosion this unit is assumed to have undergone. The definite Quarternary alluvium occurs in and adjacent to the present day stream channels. The colluvium consists of talus and landslipped blocks on the flanks of the hills and mountains.

The predominant structures in the area are a series of northeast-striking faults, of which the Cane Spring Fault is the longest. On the geologic map of Area 410, most of the faulting appears to be concentrated in the Salyer Formation and older units. There may be several reasons for this. They include: (1) these rocks are older and have been subjected to more tectonic activity, and (2) these lithologic units are thinner and more recognizable, thus faulting within them may be easier to recognize. The Ammonia Tanks member definitely appears to be less faulted than the underlying rocks. This means that much of the northeast faulting is pre-Ammonia Tanks and therefore occurred before 11 m.y. ago. This is in agreement with the end of movement along the Las Vegas Shear Zone as postulated by Longwell.[18] It should be noted

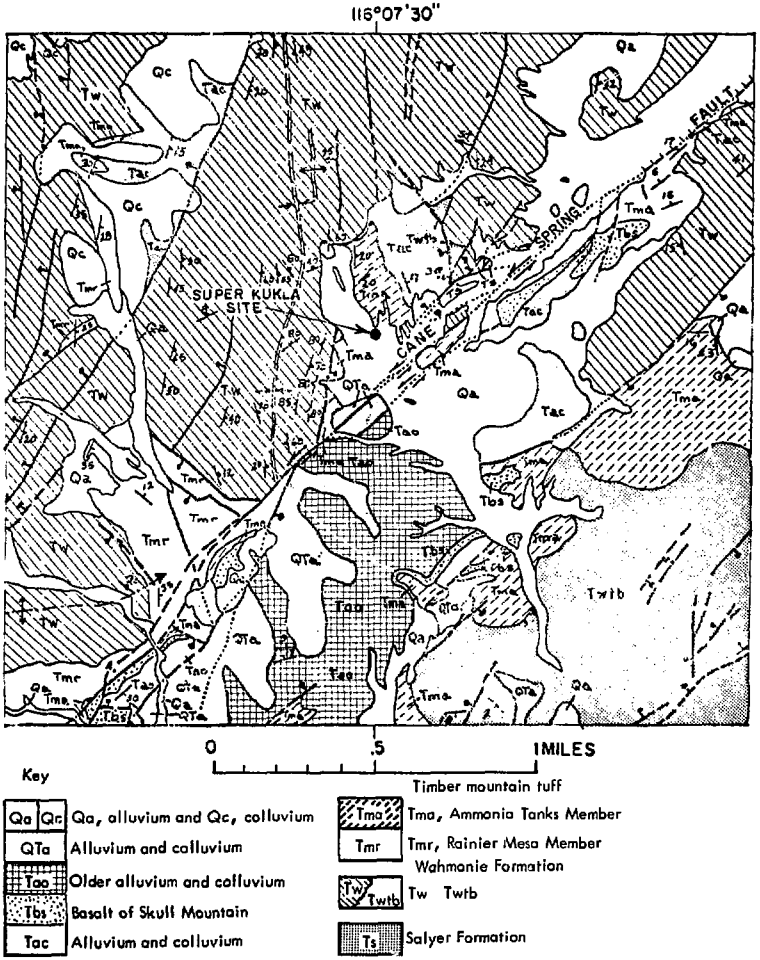

Fig. 9. Generalized geologic map of Area 410.

Table 4. Alluvium stratigraphy column in Cane Spring Quadrangle.

Geologic age	Lithology	Thickness (m)
Quaternary	Alluvium	0 - 30
	Alluvium and colluvium	0 - 150
	Older Alluvium	0 - 10
Late Tertiary or early Quaternary	Alluvium and colluvium	0 - 45
	Basalt of Skull Mountain	0 - 15
Tertiary	Alluvium and colluvium	0 - 75

that the Cane Spring Fault was active in the post-Ammonia Tanks period.

Much of the faulting on the southeast side of the Cane Spring Fault appears to have been inactive for the last 11 m.y. The Cane Spring Fault and parallel faults to the northwest offset the basalt of Skull Mountain (which is inferred to be 7 m.y. old).[23]

The age of the last movement on the Cane Spring Fault is difficult to determine. The alluvium directly overlying the basalt of Skull Mountain was offset by the Cane Spring Fault.[20] This alluvium is inferred to be Late Tertiary or very Early Quaternary. Photolineaments in alluvium parallel to the northeast extension of the Cane Spring Fault were field-checked by Ekren.[23] He could detect no displacement in either the alluvium of Cane Spring Wash or in the top few feet of underlying older alluvium.

Thus, on the basis of the displacement of sediments, we have no conclusive evidence that the fault should be considered active. However, we do have two other lines of evidence that NTS, in general, and these sites, in particular, are located in regions which are undergoing active deformation:

(1) As a result of examining a number of factors including borehole deformation, directions of crack propagation following nuclear events, seismic data, and strain measurements, Carr[5] has proposed that the NTS is undergoing extension in a N50°W - S50°E extension.

(2) Seismic evidence (Fig. 10) shows earthquake epicenters have been located as close as 5 km to the Cane Spring Fault. In addition, the Massachusetts Mountain Earthquake of August 5, 1971, occurred near the intersection of a northwest-trending structural lineament and a possible extension of the Cane Spring Fault. Although the earthquake, the fault, and the northwest-trending lineaments have an uncertain relationship, Carr[5] believes that the fault and the other features have "...been active concurrently and tend to offset one another."

Therefore, we are in the position of having a zone of significant structural weakness located in an area of active seismicity and structural deformation but of having no evidence for recent

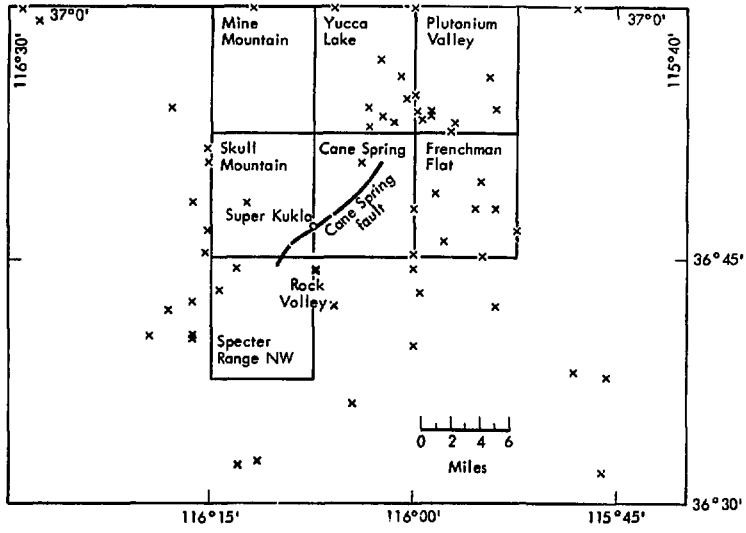

Fig. 10. Seismicity of area surrounding Super Kukla Reactor Site between 1961 and 1972.[23]

movement along the fault trace. It is our position, and that of Ekren,[23] that the continuing activity in the area together with the existing evidence of structural weakness provide sufficient evidence that the Cane Spring Fault should be considered active for seismic safety analysis purposes.

GEOLOGY OF SPECIFIC BUILDING SITES IN THE AREAS OF INTEREST

At the time of this study, there were a number of buildings of interest in the three areas. These included buildings 5100, 5120, 5130, 5140, 5310, 5318, 5319, 5320, 5325, 5400, and 5410 (Fig. 11). Our investigations of these buildings indicated that their foundations rest on either bedrock or shallow soil layers whose thickness is less than a small fraction of a wavelength for the frequencies of interest.

In general, there are numerous small faults throughout Area 410. The larger of these are shown on Fig. 11. Many small faults, which can not be adequately shown on Fig. 11, are present throughout the area. Such faults commonly have less than a meter of displacement and can be traced only for a few tens of meters.

As new buildings are considered in the area, the specific building sites will

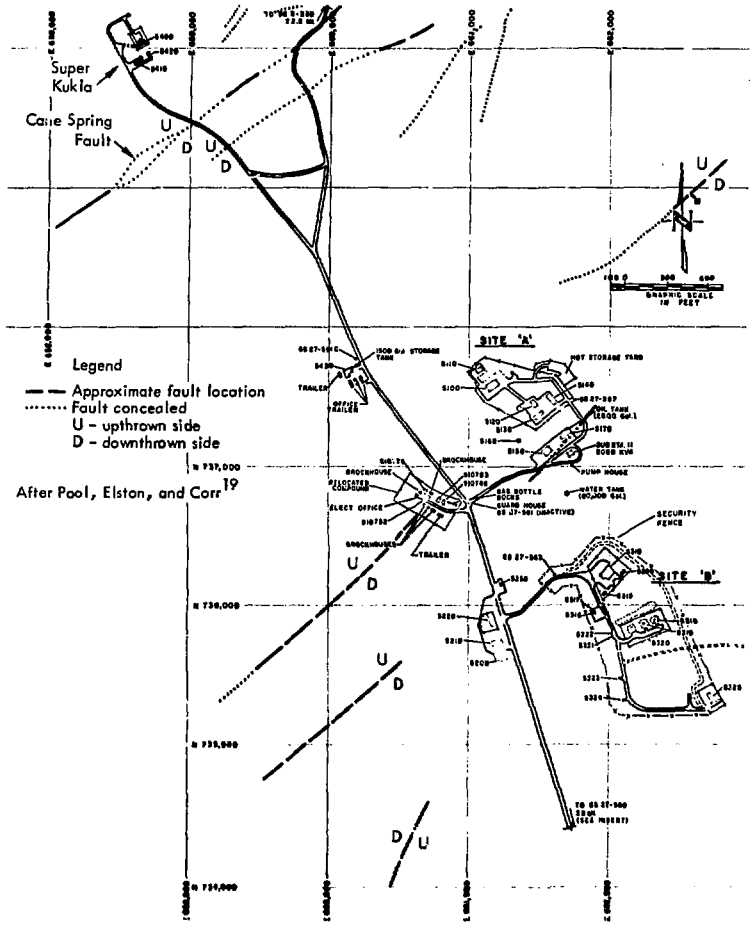

Fig. 11. Distribution of faults in vicinity of Super Kukla, Site A, and Site B.

have to be examined for the presence of these minor faults. Also the soil thickness will have to be examined. With the exceptions of these two localized features, this report should provide sufficient information for the seismic safety analysis of the proposed construction.

Regional Seismicity

The previous sections described the geologic history of NTS in general and Area 410 in particular. In the following sections, we use this information together with information about the seismicity during historic times to estimate the Safe Shutdown Earthquake (SSE), i.e., the earthquake producing the maximum vibratory accelerations at the site.[24] The characteristics of this SSE can then be used in evaluating the response of buildings at the Super Kukla Site and areas A and B (Fig. 11).

In Table 5, we list the earthquakes of magnitude 6 or greater that have occurred within historic time at distances less than about 320 km from NTS. Table 6 gives additional smaller earthquakes in the magnitude range 4.0 to 6.0 which occurred in the area 36°-37°N by 115°-116°W. These data were drawn from the articles by Slemmons et al.,[25] Ryall et al.,[26] and Gumper and Scholz[27] for the years prior to 1960 and from the work of Landers[28] for subsequent years. From these tables and from the curves of maximum acceleration versus distance from the causative fault given in Schnabel and Seed,[29] we can conclude that, except for the motion generated by the Owens Valley earthquake of 1872, Area 410 has not been subjected to peak ground accelerations in excess of 0.05 g in historic times from earthquakes within a radius of 320 km. (The Owen's

Table 5. Historic earthquakes occurring within 320 km of NTS having magnitudes ≥ 6.0.

Date	Latitude	Longitude	Magnitude	Approximate distance (km)	Descriptive name
03/26/1872	36.8	118.2	8.3	160	Owen's Valley
11/10/16	35.5	116.0	6.1	140	So. Nevada
09/18/27	37.5	118.8	6.0	255	Long Valley
12/21/32	38.8	118.0	7.2	280	Cedar Mtn.
01/30/34	38.3	118.4	6.3	270	Excelsior Mtn.
03/15/46	35.7	118.0	6.3	210	Walker Pass
04/10/47	35.0	116.3	6.4	200	Manix
12/04/48	33.0	116.3	6.5	320	Desert Hot Springs
07/23/52	35.3	118.6	6.1	280	Kern Co.
07/29/52	35.3	118.8	6.1	290	Kern Co.
08/16/66	37.4	114.2	6.1	180	So. Nevada

Table 6. Historic earthquakes occurring within the area 36°-37°N by 115°-116°W and having magnitudes in the range 4.0-6.0.

Date	Latitude	Longitude	Magnitude	Approximate distance (km)
11/10/16	36.2	116.0	–	70
03/28/34	37.3	116.6	4.5	70
03/30/34	37.7	115.3	4.9	120
03/30/34	37.7	115.3	4.0	120
03/31/34	37.7	115.3	4.0	120
04/10/36	37.1	115.6	4.0	60
06/10/36	36.6	115.5	–	60
07/28/36	37.6	115.8	4.0	90
07/28/36	37.6	115.8	–	90
07/28/36	37.6	115.8	4.5	90
07/28/36	37.6	115.8	4.0	90
11/21/39	36.5	115.0	4.0	100
03/10/40	37.5	115.0	5.0	130
03/11/40	37.0	115.0	4.5	100
04/07/40	37.0	115.0	4.5	100
05/09/40	36.2	116.2	–	70
10/12/40	37.5	115.0	–	130
06/06/41	37.1	115.8	4.0	40
09/29/54	37.5	115.8	4.4	80
03/17/55	36.2	115.2	–	100
01/28/59	36.8	116.2	4.0	10
03/27/61	36.6	116.3	4.4	30
05/07/67	37.0	115.0	4.7	100
01/06/69	37.3	116.5	4.5	70
08 10/70	37.2	115.9	4.1	50
08 05/71	36.9	116.0	4.3	15[a]
02/19/73	36.8	115.9	4.5	20[b]

[a] Massachusetts Mountain.
[b] Ranger Mountain (Frenchman Flat).

Valley earthquake could have generated peak accelerations of 0.1 g.)

Nuclear explosions are the other source of significant ground motion during historic times. Using the prediction equations given in the manual published by the Environmental Research Corporation,[30] we calculated the maximum ground acceleration from past events to be 0.04 g. We shall see that all of these historic sources are much less than the motions predicted from the SSE generated for the Cane Spring Fault.

Characterization of the Seismic Source and the Properties of the Ground Motion

In the previous section, we have considered the events occurring in historic time and have, in a sense, established a lower bound for peak acceleration of 0.1 g. To estimate the upper bound required by the definition of the SSE, we shall assume that the maximum earthquake will occur along an existing fault. This is reasonable in the sense that these zones of weakness are likely sites for new earthquakes. Furthermore, it allows us to correlate observed parameters with prior empirical studies to establish a consistent prediction process. The uncertainties are large. However, we do not see any reasonable alternative, consistent with the reactor siting guidelines.

THE METHOD USED

Wight[31] describes a process which uses the observed fault length and previous studies to estimate the maximum earthquake. Although there are a number of uncertainties, his approach provides a systematic method of addressing the problem. A brief description of the process follows. Given the total fault length, the length of rupture is estimated at one-half the observed fault length following Albee and Smith.[32] Then the works of Lieberman and Pomeroy[33] and Housner[34] relating the rupture length and the magnitude of the earthquake are used to estimate the magnitude of the SSE (see Fig. 12 which is a modified version of Wight's[31] Fig. 11). Once the magnitude of the SSE is known, the results of Schnabel and Seed[35] are used to estimate the maximum acceleration as a function of distance for a given magnitude (Fig. 13) for distances greater than 5 km.*

For distances less than 5 km a different approach is used. Some of the difficulties involved in making predictions at these short distances are discussed in Boore and Page[36] and Boore.[37] In general, we shall use an approach based on the maximum accelerations observed at similar sites.

*Although the exact value used is somewhat arbitrary, the value chosen is consistent with the lower limit of the distance for standard acceleration versus distance curves. (For an example, see Ref. 32.)

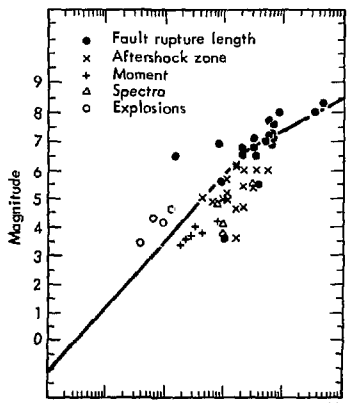

Fig. 12. Earthquake magnitude as a function of rupture length along the fault. Data is from Ref. 33 and the curve from Ref. 34.

The other quantity which we want to generate is the time history of the SSE. It can be derived from the ground motion recorded at a comparable site or from the spectra scaled from those provided in Ref. 38 if the distances are greater than 5 km. Both procedures are mentioned in Wight's report. In the event that the latter approach is used, there are standard procedures[39] for generating a synthetic seismogram having the specified response spectrum.

Finally, some attempt must be made to correct for the effect of soil if that is present. One approach for doing this is that used by Seed and Id iss.[40,41] Wight goes into more detail about the various methods used. Since soil effects are negligible in the present case, we suggest that the interested reader check Wight's work and his references.

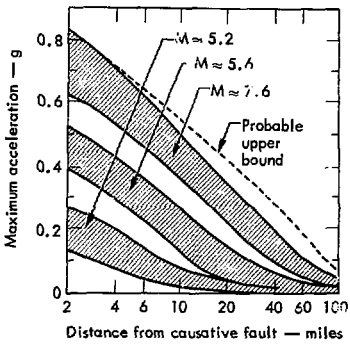

Fig. 13. Maximum acceleration as a function of distance for given magnitudes.[35]

HISTORICAL OBSERVATIONS OF LARGE ACCELERATIONS

Since we are interested in predicting the properties of the SSE, which, by definition, is concerned with the maximum vibratory acceleration, it is worthwhile to specifically examine some of the larger accelerations that have been observed in the western U.S. Wight does this in his report to some extent, but the importance of the subject makes a repetition worthwhile. In general, the value of the observed peak acceleration has risen as the number of strong motion instruments has increased. Prior to 1966, the highest ground accelerations (0.3 g) had been recorded during the El Centro, California, earthquake of May 18, 1946, and the Olympia, Washington, earthquake of April 13, 1949.

In 1966, a magnitude 5.5 earthquake occurred on the San Andreas Fault near Parkfield, California. It was accompanied by surface breakage along approximately 32 km of the fault. A number of seismic stations had been emplaced in a line across the fault at the time of the earthquake. Properties of selected stations in this array are given in Table 7 using data from Cloud and Perez.[42] The immediate consequence of the N65E measurement at Station 2 was to raise the maximum observed peak acceleration to 0.5 g. In addition, the missing record from the instrument N25W took on added importance both because of the possibility that it might have recorded even larger accelerations and because the peak acceleration should be determined from the vector sum of the two horizontal

Table 7. Selected station and acceleration data for the Parkfield earthquake.

Station name	Distance to fault (km)	Foundation	Orientation	Peak acceleration (g)
Temblor	6.4	Alluvium	N65W	0.27
			vertical	0.16
			S25W	0.40
2	0.1	Alluvium	N65E	0.50
			vertical	0.35
			N25W	Missing
5	5.3	Alluvium	N85E	0.46
			vertical	0.18
			N5W	0.40

components.* An initial investigation by Housner and Trifunac[43] using a seismoscope record from Station 2 indicated that the acceleration on the component oriented N25W was stronger than the 0.5 g recorded on the component oriented N65E. This was consistent with the fact that the fault exhibits right lateral strike slip motion along a trend N25° - 40°W which is nearly parallel to the direction of motion measured by the N25°W accelerometer. Later, Trifunac and Hudson[44] were able to reconstruct the missing component using a seismoscope record from the same area. The reconstruction indicated that the missing component was 25-30 % higher than the one which had been recorded. The combined components indicate a peak acceleration of 0.7 to 0.8 g rather than the 0.5-g maximum which is usually cited from the examination of the N65°E record. Although Station 2 was located on alluvium, there are indications[42] that soil amplification effects are negligible in the period range of interest.

Further support to these values of high ground acceleration was provided by the record made by the accelerometer at Pacoima Dam during the San Fernando, California earthquake (magnitude 6.6) of February 9, 1971. The recording site was about 4 km from the surface rupture associated with motion on the Tujunga Thrust Fault. The surface rupture is about 15 km in length and the dam is located at about the center of the rupture. The topography is quite rugged and the accelerometer was located on a rocky spine extending out into the valley containing the Pocoima Dam.[44] During the earthquake, several cycles of acceleration in the range 0.6 - 0.7 g were observed early in the record and one peak of 1.25 g was observed on each component later in the record (see Fig. 14).[44] From the vector sum of the components, we conclude that the site was subjected to peak accelerations similar to 1 g early in the disturbance and as high as 1.6 g later. Several explanations of these high accelerations have been put forward. These involve

*However, note that it seems to be customary practice to use merely the largest component of acceleration which has been recorded, not the vector sum which represents the true maximum acceleration. The main reasons for this appear to be related to matters of convenience and have little or no technical justification.

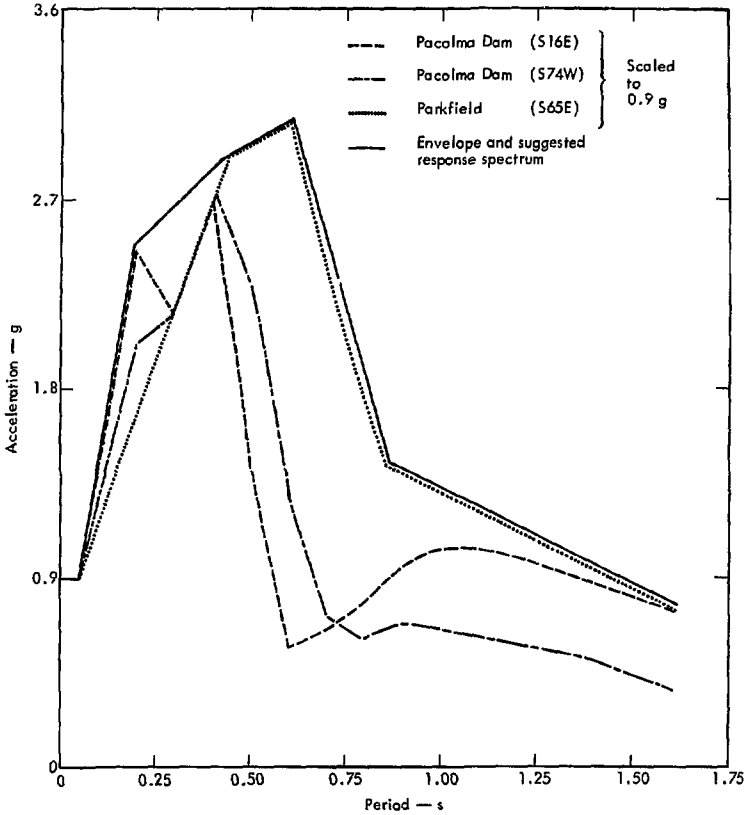

Fig. 14. Scaled and suggested horizontal response spectra for Area 410 seismic safety analysis.

effects due to a combination of localized rupture effects and low attenuation in the hard rock material at the site[45] and site topography.[46-48] Two of the latter articles, Refs. 46 and 48, are based on numerical modeling of the area around the dam. They obtain reductions in peak acceleration from 1.25 g to 0.73 and 0.40 g, respectively, as a result of filtering and correction for the topography. The other article[41] used measurements made at the damsite and surrounding areas for eight

aftershocks to compute empirical topographic corrections. These gave reductions in the peak g-levels of the components from 1.25 to 0.89 g or 0.76 g depending on the component. Because of the uncertainties in the numerical modeling involved in the other two studies, we tend to give greater weight to this empirical investigation. We use an average reduction factor of 0.65 to correct for the topographic amplification of the vector sum. This gives a corrected peak vector acceleration of 1.0 g.

In addition to the observational evidence, a number of "order of magnitude" calculations[49, 50] indicate that there is no theoretical reason why peak accelerations greater than 1 g cannot occur. Furthermore, a number of references[24, 36, 37, 51] indicate that the behavior of the near fault region (2-5 km) cannot be described by an extrapolation of curves based on data from distances greater than 5 km. Also, these references indicate that there is only a rough correlation of peak acceleration with either magnitude or geology in the fault region. These conclusions are in agreement with the intuitive feeling that the peak close-in effects should depend on such things as the shear strength of the material, the stress drop, the attenuation, and the nature of the fracture zone. Further, we expect the effects of fault geometry to be important at short distances.

In summary, we have the following observational evidence regarding the ground motion at sites less than 5 km from the fault zone:

- Single peaks as high as 1.6 g have been recorded in the vector ground accelerations in areas with large topographic relief. Even after applying an empirical correction factor of 0.65 on the basis of observations made by Mickey, Perez, and Cloud,[47] we have a corrected, vector ground acceleration with a peak of 1.0 g.
- Vector ground accelerations with single peaks near 0.8 g have been observed in less rugged areas.
- The component peak acceleration at short distances is only roughly correlated with the magnitude of the earthquake.
- Predictions for distances less than 5 km cannot be made on the basis of curves constructed from measurements made at larger distances.

THE SAFE SHUTDOWN EARTHQUAKE

Recognizing the many uncertainties inherent in the process, we can now use the prediction process outlined in the preceding sections and the cited references to obtain an estimate of the peak accelerations and the safe shutdown earthquake for Area 410 at NTS. In Table 8, we list the various faults which have been identified out to a distance of 320 km and give various observed and derived properties.[52-55] As previously discussed, we have considered all of the faults in the immediate area to be active. Since all of the buildings of interest are within less than 2 km of each other, we have used a single distance to the faults for all of the buildings. In general, the magnitudes were computed by the method described previously. The Owens Valley, the Cane Spring, and the Massachusetts Mountain - Cane Spring Complex values are exceptions to this. For the Owen's Valley result, we used the historically observed magnitude of 8.3

Table 8. Observed and derived properties of major faults within 320 km of Area 410 at NTS.

Fault	Distance to fault (km)	Length of fault (km)	Maximum rupture length (km)	Past displacement (km)	Magnitude[a]	Peak acceleration (g)[b]	Remarks
Cane Spring	0.2	16-18	8-9	1.6-4.8	5.8	0.9[c]	One of a series of left-lateral in echelon faults associated with Las Vegas Shear Zone.[20]
Massachusetts Mountain	9.0	1.6-8	0.8-4	1.6	5.3	0.2	A series of NE and NW striking faults. Possible extension of the Cane Spring Fault. Massachusetts Mountain earthquake (mag 4.3) occurred 8/5/71 near junction with Cane Spring.
Massachusetts Mountain plus Cane Spring	0.2	18-26	9-13	1.6-4.8	6.1	0.9[c]	This gives an estimate of the combined system.[5]
Yucca	14	24-32	12-16	0.2	6.5	0.4	A right laterial fault with some vertical displacement.[5]
Las Vegas	16	130	65	64	7.0	0.5	Major regional feature with right lateral slip.[5, 15]
Furnace Creek-Death Valley	64	300	150	80	7.5	0.2	Recent movement on some associated faults.[8, 52]
Garlock	130	240	120	20	7.4	0.05	Active slip movement during recent times.[53, 54]
Owens Valley	160	180	90		8.3[d]	0.1	Large earthquake associated with fault in 1872.
White Wolf	260	70	35	3 (vertical)	7.2	<0.05	Reverse fault. Recent earthquake activity.[53]
San Andreas	310	960	480	105-560	8.2	<0.05	Ref. 55.

[a]Estimated from Fig. 12 and the maximum rupture length unless otherwise noted.

[b]Estimated from Fig. 13, the magnitude and the distance unless otherwise noted.

[c]Estimated from Pacoima Dam and Parkfield *spectra suitably scaled.*

[d]Historic maximum.

associated with the 1872 earthquake and calculated the acceleration from Fig. 13.

We can expect that the ground motion appropriate for sites near the Cane Spring Fault and the Massachusetts Mountain – Cane Spring Complex Fault could be as great as that experienced at sites near the San Fernando and Parkfield earthquakes. These had corrected peak vector accelerations of 1.0 g and 0.8 g, respectively. However, the earthquake magnitude for the Cane Spring Fault (5.8-6.1) is intermediate to those of the San Fernando (magnitude 6.6) and Parkfield (magnitude 5.5) earthquakes. Therefore, we choose the intermediate value of 0.9 g as being appropriate for the peak acceleration to be associated with the SSE occurring on these faults.

Finally, we are left with the problem of determining the response spectra to be used for the SSE. In general, the effect of attenuation suggests that two different response spectra be generated. One, for close-in earthquakes of moderate size, would be rich in high-frequency components. The other, for very large, distant earthquakes, would be relatively rich in low-frequency components. However, in the present case, the effects of the large earthquakes at distance are secondary to those of the projected magnitude 5.8-6.1 earthquake on the Cane Spring – Massachusetts Mountain Faults. Therefore, we will use the spectra developed for these faults with proper scaling as described below.

In Fig. 14, we give the horizontal response spectrum estimated for Area 410. The response spectrum is the envelope of the two components of the Pacoima Dam records (Fig. 15), the San Fernando earthquake, and the N65°E component of the Station 2 record for the Parkfield earthquake (Fig. 16), all scaled to 0.9 g. Data were obtained from Refs. 56 and 31, respectively.

Although the spectrum is reasonable in view of the accepted engineering practice [compare, for example, a curve (not shown) constructed for 0.7 g by the methods of Refs. 38 and 57], we believe that present practice places undue emphasis on the zero period value in the spectrum. At one point we considered scaling on the basis of the average of the highest of four peak accelerations. This approach has the merit of reducing the emphasis placed on a single peak (see Ref. 35, for some comments on the dependence of spectra on single peaks). It gave spectra which were about 10% higher and gave closer agreement between the Parkfield and Pacoima Dam spectra. However, since we consider 10% variation to be within the uncertainty of the present curve, since the present curve corresponds to accepted practice, and since we are not in a position to justify a new approach at this time (although we believe a new approach should be developed), we present the results of Fig. 14.

To obtain an estimate of the response spectrum for the vertical displacement, we suggest the procedure relating the horizontal and vertical spectra given in Ref. 38. In general, the suggested vertical response spectra values are two-thirds those of the horizontal spectra for periods greater than 4 s; for periods less than 0.3 s, they are the same; and for periods between 0.3 and 4 s, the ratio varies from two-thirds to one.

The values for the Operating Basis Earthquake are strictly speaking the

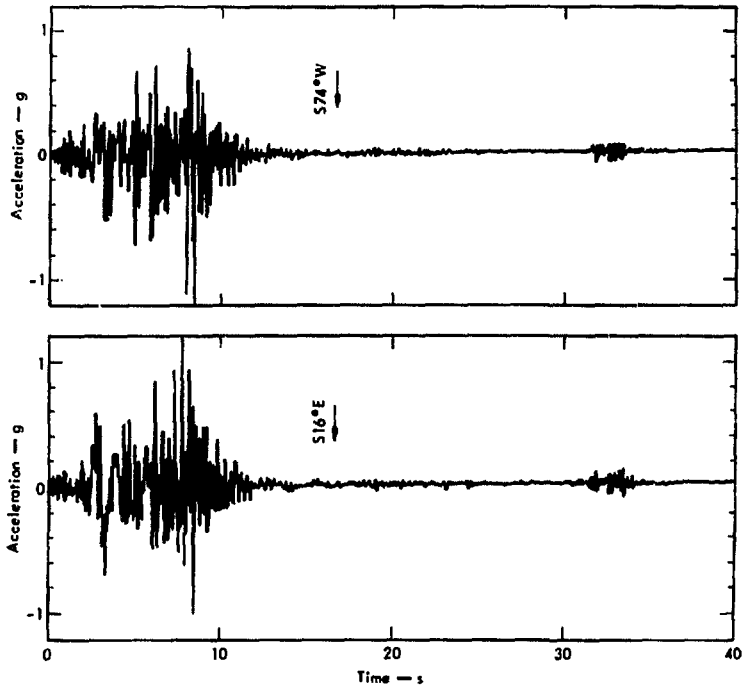

Fig. 15. Plot of accelerograms recorded at the strong motion site adjacent to Pacoima Dam.[44]

province of the design engineer. We note that common practice is to use an Operating Basis Earthquake corresponding to one-half the SSE.

In general, spectra determined in this way should be corrected for soil amplification. However, since the buildings in question are sited on bedrock or, at most, one to two meters (less than a small fraction of a wavelength) of alluvium, there is no need to correct the soil layer for the

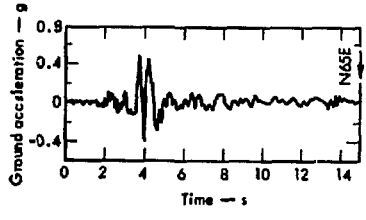

Fig. 16. Plot of accelerogram recorded at strong motion Site No. 2 for the Parkfield earthquake.

purpose of determination of the seismic motion. However, the presence of such a layer of alluvium is of possible importance in the interaction of the soil and the foundation.

Finally, we consider the relative displacements to which the buildings might be subjected by faulting. The Cane Spring Fault is an obvious zone of weakness in the earth's crust and the whole area must be considered to be subject to significant tectonic stress and to be in a zone of continuing seismic activity.[5,6] Faulting associated with this zone of weakness could occur anywhere along a broad zone including the region occupied by the buildings of interest. Using the results of Chinnery,[58] we find a relative displacement of 0.2-0.5 m (at the +1σ level) across the fault trace for an earthquake of magnitude 5.8-6.1. This is less than the 1-2 m value considered reasonable by Ekren.[23] The corresponding vertical displacement is estimated to be about one-third of the horizontal displacement.[22]

Summary

In response to the ERDA request that critical buildings in Area 410 at NTS be evaluated in a safety analysis report, we conducted a geological and seismological investigation of the area. We considered those factors necessary to meet the requirements of Sec. 2.5 of the ERDA standard guidelines.[24]

In particular, we reviewed the regional and local geology at the site, identified potential seismic sources, estimated the peak acceleration and SSE characteristics appropriate for the bedrock and shallow alluvium locations of the buildings, and estimated the peak relative displacement. Because of the size and proximity of the Cane Spring Fault, we arrived at a prediction of a peak acceleration of 0.9 g for the site. The corresponding response spectrum for the SSE is given in Fig. 14. The primary bases for these conclusions were the requirement that maximum values were to be predicted and the fact that values of peak acceleration of this size have, in fact, been observed. The response spectrum was determined from the envelope of records from the San Fernando and Parkfield earthquakes, suitably scaled. Finally, a maximum relative displacement across the Cane Spring Fault of 0.2 to 0.5 m was estimated as being appropriate for the site on the basis of a magnitude 5.8-6.1 earthquake.

Acknowledgments

We thank Larry Wight of LLL for his many useful discussions and his calculations of some of the response spectra. Without his knowledge and assistance, our work would have been considerably more difficult. Our thanks also to R. D. McArthur (LLL-N) for spot checking some field relationships in Area 410 and for

discussing some aspects of Area 410 geology. We also thank William Quinlivan, Frank Byers, Jr., and E. B. Ekren of the Special Projects Branch, U. S. Geologic Survey, for reviewing the geologic portion of this report.

References

1. C. B. Hunt, Physiography of the United States (W. H. Freeman and Co., San Francisco, Cal., 1967).
2. P. B. King, The Tectonics of North America – A Discussion to Accompany the Tectonic Map of North America, Scale 1:5,000,000, U. S. Geological Survey, Washington, D. C., Professional Paper 628 (1969).
3. J. H. Stewart, Geol. Soc. Am. Bull. 83, 1345 (1972).
4. E. B. Ekren, C. L. Rogers, R. E. Anderson, and P. O. Orkild, "Age of Basin and Range Faults in Nevada Test Site and Nellis Air Force Range Nevada," in Nevada Test Site, Memoir 110, E. G. Eckel, Ed. (Geological Society of America, Boulder, Colo., 1968), pp. 247-250.
5. W. J. Carr, Summary of Tectonic and Structural Evidence for Stress Orientation at the Nevada Test Site, U. S. Geological Survey, Washington, D. C., Rept. USGS-474-181 (1974).
6. E. B. Ekren, "Geologic Setting of Nevada Test Site and Nellis Air Force Range," in Nevada Test Site, Memoir 110, E. B. Eckel, Ed., (Geological Society of America, Boulder, Colo., 1968), pp. 11-19.
7. J. Gilluly, Volcanism, Tectonism, and Plutonism in the Western United States (Geological Society of America, Boulder, Colo., 1965), Spec. Paper 80.
8. L. A. Wright, B. W. Troxel, E. G. Williams, M. T. Roberts, and P. E. Diehl, "Precambrian Sedimentary Environments of the Death Valley Region, Eastern California," in Guidebook: Death Valley Region, California and Nevada (Death Valley Publishing Co., Shoshone, Cal., 1974).
9. M. W. Reynolds, "Geology of the Grapevine Mountains, Death Valley, California: A Summary," in Guidebook: Death Valley Region, California and Nevada (Death Valley Publishing Co., Shoshone, Cal., 1974).
10. H. Barnes and F. G. Poole, "Regional Thrust-Fault System in Nevada Test Site and Vicinity," in Nevada Test Site, Memoir 110, E. B. Eckel, Ed. (Geological Society of America, Boulder, Colo., 1968) pp. 233-238.
11. B. D. Burchfield, P. J. Pelton, and J. Sutter, Geol. Soc. Am. Bull. 81, 211 (1970).
12. R. J. Fleck, Geol. Soc. Am. Bull. 81, 2807 (1970).
13. J. H. Stewart, Geol. Soc. Am. Bull. 82, 1019 (1971).
14. R. L. Armstrong, E. B. Ekren, E. H. McKee, and D. C. Noble, Am. Jour. Sci. 267, 478 (1969).
15. M. L. Silberman and E. H. McKee, Isochron/West, No. 4, 7 (1972).
16. E. H. McKee, Geol. Soc. Am. Bull. 82, 3497 (1971).
17. R. F. Marvin, F. M. Byers, Sr., H. H. Mehnert, P. P. Orkild, and T. W. Stern, Geol. Soc. Am. Bull. 81, 2657 (1970).
18. C. R. Longwell, Geol. Soc. Am. Bull., 85, 985 (1974).

19. F. G. Poole, D. P. Elston, and W. J. Carr, Geologic Map of the Cane Spring Quadrangle, Nye County Nevada, U. S. Geol. Survey Geol. Quad. Map GQ 455 (1965).
20. E. B. Ekren and K. A. Sargent, Geologic Map of Skull Mountain Quadrangle, Nye County Nevada, U. S. Geol. Survey Geol. Quad. Map GQ-387 (1965).
21. E. N. Hinrichs, Geologic Map of the Camp Desert Rock Quadrangle, Nye County Nevada, U. S. Geol. Survey Geol. Quad. Map GQ-726 (1968).
22. K. A. Sargent and J. H. Stewart, Geologic Map of the Specter Range NW Quadrangle, U. S. Geol. Survey Geol. Quad. Map GQ 884 (1971).
23. E. B. Ekren, Geologic Examination of the Super Kukla Reactor Site, Nevada Test Site, U. S. Geol. Survey, Washington, D. C., Rept. USGS 474-161 (1972).
24. USAEC Regulatory Staff, Standard Format and Content of Safety Analysis Reports for Nuclear Power Plants, Rev. 1, (October 1972) pp. 2.5-7.
25. D. B. Slemmons, A. E. Jones, and J. I. Gimlett, Bull. Seis. Soc. Am. 55, 519 (1965).
26. A. Ryall, D. B. Slemmons, and L. D. Gedney, Bull. Seis. Soc. Am. 56, 1105 (1966).
27. F. J. Gumper and C. Scholz, Bull. Seism. Soc. Am. 61, 1413 (1971).
28. J. F. Landers, "Seismological Notes," a regular feature, in Bull. Seism. Soc. Am. (1961-1974).
29. P. B. Schnabel and H. B. Seed, Bull. Seism. Soc. Am. 63, 501 (1973).
30. Environmental Research Corporation, Prediction of Ground Motion Characteristics of Underground Nuclear Detonations, U. S. ERDA, Nevada Operations Office, Las Vegas, Rept. NVO-1163-29 (1974).
31. L. H. Wight, A Geological and Seismological Investigation of the Lawrence Livermore Laboratory Site, Lawrence Livermore Laboratory, UCRL-51592, Rev. 1 (1974).
32. A. L. Albee and J. L. Smith, "Earthquake Characteristics and Fault Activity in Southern California," in Engineering Geology in Southern California (L. A. Section, Assoc. of Engrg. Geologists), R. Lung and R. Proctor, Eds. (1966), pp. 9-44.
33. R. C. Lieberman and P. W. Pomeroy, Bull. Seism. Soc. Am. 60, 879 (1970).
34. G. W. Housner, "Engineering Estimates of Ground Shaking and Maximum Earthquake Magnitude," in Proc. 4th World Conf. Earthquake Engrg. (Editorial Universitaria, Santiago, Chile, 1969), pp. 1-13.
35. P. B. Schnabel and H. B. Seed, Bull. Seis. Soc. Am. 63, 501 (1973).
36. D. M. Boore and R. A. Page, Accelerations Near Faulting in Moderate-sized Earthquakes, U. S. Geological Survey open file report.
37. D. M. Boore, "Empirical and Theoretical Study of Near Fault Propagation in Proc. 5th World Conf. Earthquake Engrg. (Ministry Public Works, Rome, Italy, 1973), No. 301a.
38. Design Response Spectra for Seismic Design of Nuclear Power Plants, USAEC Regulatory Guide 1.60 (USAEC, Washington, D. C., 1973).

39. G. W. Housner and P. C. Jennings, ASCE J. Engrg., Mech. Div. 90 (EM1), 113 (1964).
40. H. B. Seed and I. M. Idriss, J. Soil Mech., Found. Div., ASCE 95(SM5), 1199 (1969).
41. H. B. Seed and I. M. Idriss, Soil Moduli and Damping Factors for Dynamic Response, University of California, Berkeley, Rept. EERC-70-10 (1970).
42. W. K. Cloud, and V. Perez, Bull. Seism. Soc. Am. 57, 1179 (1967).
43. G. W. Housner and M. D. Trifunac, Bull. Seism. Soc. Am. 57, 1193 (1967).
44. M. D. Trifunac and D. E. Hudson, Bull. Seism. Soc. Am. 61, 1393 (1971).
45. B. A. Bolt, Bull. Seism. Soc. Am. 62, 1053 (1972).
46. D. M. Boore, Bull. Seism. Soc. Am. 63, 1603 (1973).
47. W. V. Mickey, V. Perez, and W. K. Cloud, "Amplification Studies of the Pacoima Dam from Aftershocks of the San Fernando Earthquake," in Proc. 5th World Conf. Earthquake Engrg.(Ministry of Public Works, Rome, Italy,1973), No. 86.
48. R. B. Reimer, R. W. Clough, and J. M. Raphael, "Evaluation of the Pacoima Dam Accelerogram," in Proc. 5th World Conf. Earthquake Engrg. (Ministry of Public Works, Rome, Italy 1973), No. 293.
49. J. N. Brune, J. Geophys. Res. 75, 4997 (1970).
50. Y. Ida, Bull. Seism. Soc. Am. 63, 959 (1973).
51. N. C. Donovan, "A Statistical Evaluation of Strong Motion Data Including the February 9, 1971 San Fernando Earthquake," in Proc. 5th World Conf. Earthquake Engrg. (Ministry of Public Works, Rome, Italy, 1973) No. 155.
52. L. A. Wright, and B. W. Troxel, Geol. Soc. Am. Bull. 78, 933 (1967).
53. J. P. Buwalda, "Geology of the Tehachapi Mountains, California," in Geology of Southern California, Bulletin 170, R. H. Jahns, Ed. (California Division of Mines, Sacramento, Cal., 1954).
54. D. F. Hewett, "General Geology of the Mojave Desert Region, California," in Geology of Southern California, Bulletin 170, R. H. Jahns, Ed. (California Division of Mines, Sacramento, Cal., 1954).
55. L. F. Noble, "The San Andreas Fault Zone from Soledad Pass to Cajon Pass, California," in Geology of Southern California, R. H. Jahns, Ed. (California Division of Mines, Sacramento, Cal., 1954).
56. P. C. Jennings, Ed., Engineering Features of the San Fernando Earthquake, February 9, 1971, Earthquake Engineering Research Laboratory, California Institute of Technology, Pasadena, Cal., Rept. 71-02 (1971).
57. John Blume and Associates, Recommendations for Shape of Earthquake Response Spectra, USAEC, Rept. WASH-1254 (1973).
58. M. A. Chinnery, Bull. Seism. Soc. Am. 59, 1969 (1969).

MBB/jd/la